

Supplementary material for

Computational Screening of Doped Graphene

Electrodes for Alkaline CO₂ Reduction

Anand M. Verma, Karoliina Honkala,* and Marko M. Melander*

Nanoscience Center, P.O. Box 35 (YN) FI-40014, Department of Chemistry, University of Jyväskylä, Finland

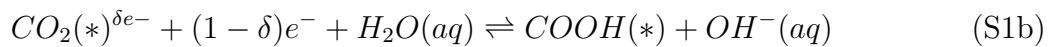
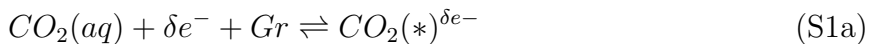
E-mail: karoliina.honkala@jyu.fi; marko.m.melander@jyu.fi

Derivation of free energies for simultaneous and decoupled PCET reactions

Here thermodynamic relations used in the main paper are derived. Expression for both decoupled electron (ET)/proton transfer (PT) steps and concerted proton-coupled electron transfer (PCET) steps are developed.

The reaction mechanism and needed thermodynamic identities

We consider the following reaction steps





Next the free energy for each step is derived. We will need the following basic thermodynamic identities and considerations.

- Gibbs energy is $G = \sum_i \tilde{\mu}_i n_i$. For the proton the chemical potential is $\tilde{\mu}_{H^+} = \mu_{H^+} + \phi^S - k_B T \ln 10 \times pH$ where ϕ^S is the (local) electric potential in solution.
- The water dissociation energy is $K_w = \exp[-\Delta G_w / k_B T]$ with $\Delta G_w = \tilde{\mu}_{H^+} + \tilde{\mu}_{OH^-} - \mu_{H_2O}$. The water dissociation free energy is obtained from standard electrochemical tables and at pH=14 $\Delta G_w = 0.83$ eV.¹
- The absolute electrode potential in the vacuum scale is $U_{abs} = -\tilde{\mu}_e = -(\mu_e - \phi^M) = -eE_F$ where ϕ^M is the electrostatic potential in the electrode. Reference against the standard hydrogen electrode (SHE) is obtained as $U(SHE) = -\tilde{\mu}_e^{ABS} - (-\tilde{\mu}_e^{SHE}) = U_{ABS} - U_{ABS}^{SHE}$.^{2,3}
- The computational hydrogen electrode (CHE)⁴ is defined from the reaction



The free energy for this reaction is $\Delta G_{CHE} = 1/2\mu_{H_2} - \tilde{\mu}_{e^-} - \tilde{\mu}_{H^+} = 1/2\mu_{H_2} - \tilde{\mu}_{e^-}^0 + \Delta\phi - \mu_{H^+}^0 + k_B T \ln 10 \times pH = +\Delta\phi + k_B T \ln 10 \times pH$ where $1/2\mu_{H_2} - \tilde{\mu}_{e^-}^0 - \mu_{H^+}^0 = 0$ by definition at $U = 0$ vs. SHE and pH=0. With these definitions the reaction energy on the SHE/CHE scale becomes $\Delta G(SHE) = U(SHE) + k_B T \ln 10 \times pH$

- The SHE scale is converted to the RHE scale by subtracting the pH term
- We note that while the OH^- and H^+ species appear in the developed and utilized extended thermodynamics cycles, the (free) energy of neither species has been explicitly used or evaluated as they cancel in the final equations S9 and S12.

Step 1: Electrosorption of CO₂

The reaction free energy of the CO₂ adsorption in step (S1a) is formally

$$\Delta G_1 = \tilde{\mu}_{CO_2^{\delta-}(*)} - G(Gr) - \mu_{CO_2(g)} - \delta\tilde{\mu}_e \quad (S3)$$

The chemical potentials of gaseous and solvated species in equilibrium are equal, therefore, we can select either the gas phase or the solution phase chemical potential. Here, in this work, we have chosen to use the gaseous CO₂ at NTP conditions as the reference state.

However, it can be shown⁵ that dividing the charge between the catalyst and the adsorbate is superficial as the charge transfer depends on the utilized model. In particular, the thermodynamics from the Gibbs adsorption equation remain unchanged on whether the adsobate and catalysts are treated as a single constituent or as separate species.⁵ Therefore the species' surface excess free energy determining the free energy change is independent on whether or not charge transfer takes place as only the total surface charge of the electrode and the adsorbed species can be determined.

To account for the effect of the electrode potential on the adsorption energy, a recent study⁶ utilized a dipolar model for CO₂ and adsorption was taken to depend on the electrode potential as $\Delta G(U)_{CO_2} = \Delta G_0 + \nu \vec{\mathcal{E}}(U) | -\frac{\alpha |\vec{\mathcal{E}}(U)|^2}{2}$ where ΔG_0 is the reference adsorption energy at $U = 0$ vs SHE, $\vec{\mathcal{E}}(U)$ is the electric field felt by the adsorbed CO₂ as a function of the potential, ν is the dipole moment, and α is the polarizability. In this model, the $\Delta G(U)_{CO_2}$ has a linear dependence on U with a slope depending on the electrode material under the assumptions used in Ref. 6 . Another thermodynamically well-defined way to include the potential dependency in the adsorption energy is obtained through the use of the electrosorption valency,⁵ $\gamma(U)$. Unlike Schmickler and Guidelli,⁵ we have included the potential dependence in the definition of the electrosorption valency because the (CO₂) adsorption energy may depend non-linearly on the electrode potential. Including the potential dependency in the electrosoprtion valency gives

$$\gamma(U) = \left(\frac{\partial \Delta G^{ads}(U)}{\partial U} \right)_{\Gamma_i} \quad (S4)$$

where Γ_i denotes the surface excess of all species. Using the CO₂ adsorption free energy at some reference potential, $\Delta G_1(U_{ref})$, the effect of changing the potential maybe computed using the electrosorption valency. For the ease of calculation, we assume that the electrosorption valency is independent of the potential ($\gamma(U) \approx \gamma$) - this assumption should be valid close to the reference potential but will deteriorate for potentials $|U| >> |U_{ref}|$. With the assumption, the adsorption energy as a function of the electrode potential is

$$\Delta G_1(U) = \Delta G_1(U_{ref}) + \gamma \times (U - U_{ref}) \quad (S5)$$

The reference potential is chosen on the SHE scale and set to zero. This defines the free energy change as

$$\Delta G_1(U_{SHE}) = \Delta G_1(U(SHE) = 0) + \gamma \times U(SHE) \quad (S6)$$

Step 2: PT and partial ET

To facilitate the use of the CHE model, step (S1b) is separated to three steps using a thermodynamic cycle in Fig. S1

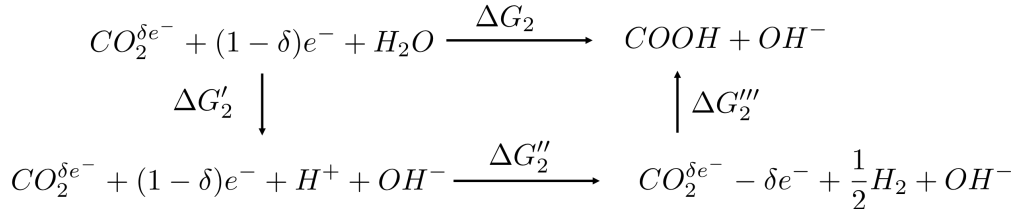


Figure S1: Thermodynamic cycle for step 2.

The first substep is the water dissociation step and the free energy change for this steps was given in above: $\Delta G'_2 = \Delta G_w$. The second substep is the hydrogen evolution step which we take on the SHE scale using the CHE model. The free energy change for this step also

discussed above and results in: $\Delta G''_2 = U(SHE) + k_B T \ln 10 \times pH$. The final substep is the formation of the adsorbed carboxyl species and the free energy is formally

$$\Delta G'''_2 = \mu_{COOH(*)} - \frac{1}{2}\mu_{H_2} - \tilde{\mu}_{CO_2^{\delta e-}(*)} - \delta\tilde{\mu}_e \quad (S7)$$

where $\mu_{COOH(*)}$ indicates the free energy of the COOH-graphene adsorption complex. As discussed for Step 1, $\tilde{\mu}_{CO_2^{\delta e-}(*)}$ is thermodynamically indistinguishable from the $\tilde{\mu}_{CO_2(*)} + \delta\tilde{\mu}_e$. Therefore, we can replace the chemical potential $CO_2(*)$ with adsorption energy at some reference potential and account the electrode potential using the electrosorption valency discussed in relation to Step 1. This leads to

$$\Delta G'''_2 = \mu_{COOH(*)} - \frac{1}{2}\mu_{H_2} - \mu_{CO_2(*,U(SHE)=0)} - \gamma \times U(SHE) \quad (S8)$$

Then, the free energy change of step 2 is

$$\begin{aligned} \Delta G_2 &= \Delta G'_2 + \Delta G''_2 + \Delta G'''_2 \\ &= \Delta G_w + \mu_{COOH(*)} + (1 - \gamma)U(SHE) + k_B T \ln 10 \times pH \\ &\quad - \frac{1}{2}\mu_{H_2} - \mu_{CO_2(*,U(SHE)=0)} \end{aligned} \quad (S9)$$

Steps 1+2: Concerted PCET

If the ET and PT take place in one concerted step, the free energy change is simply

$$\begin{aligned} \Delta G_{1+2} &= \Delta G_1 + \Delta G_2 \\ &= \Delta G_w + \mu_{COOH(*)} + U(SHE) + k_B T \ln 10 \times pH \\ &\quad - \frac{1}{2}\mu_{H_2} - \mu_{CO_2(*,U(SHE)=0)} \end{aligned} \quad (S10)$$

which is the same as derived from the traditional CHE model for concerted PCET, as it

should be.

Step 3: Concerted PCET

For this step the thermodynamic cycle in Fig S2 is utilized. The addition of water on both sides of the total reaction does not affect the total thermodynamics but facilitates the use of the CHE model.

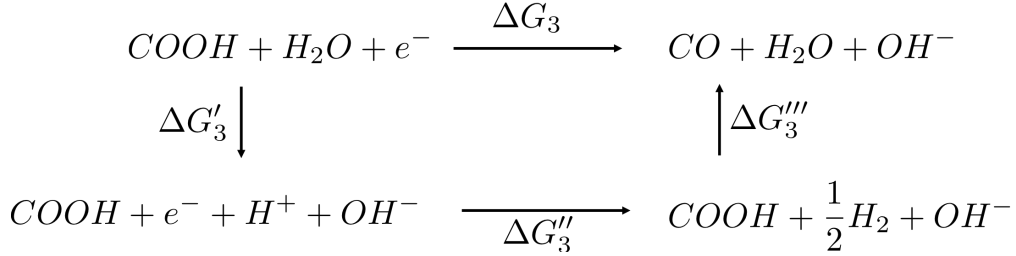


Figure S2: Thermodynamic cycle for step 3.

The first substep is the water dissociation reaction for which the free energy change is $\Delta G'_3 = \Delta G_w$. The second substep is again the hydrogen evolution step which we take on the SHE scale and employ the CHE model. The free energy change for this step is also discussed in relation to Eq. 2 and yields: $\Delta G''_3 = U(SHE) + k_B T \ln 10 \times pH$. The final substep is the formation of CO and the free energy change is obtained using CHE

$$\Delta G'''_3 = \mu_{CO(*)} + \mu_{H_2O} - \frac{1}{2}\mu_{H_2} - \mu_{COOH(*)} \quad (S11)$$

The free energy change of step 3 is then

$$\begin{aligned}
 \Delta G_3 &= \Delta G'_3 + \Delta G''_3 + \Delta G'''_3 \\
 &= \Delta G_w + U(SHE) + k_B T \ln 10 \times pH + \mu_{CO(*)} + \mu_{H_2O} - \frac{1}{2}\mu_{H_2} - \mu_{COOH(*)}
 \end{aligned} \quad (S12)$$

Sources of thermodynamic parameters

In this section, we present the methodology to calculate the contributions of entropy and energy resulting from translational, rotational, electronic and vibrational components. Each calculation starts with the calculation of partition function (q), which will be utilized to compute the thermodynamic entropy, enthalpy and free energy.

Partition functions

The total partition function (q_{tot}) is a product of partition functions of translational (q_t), rotational (q_r), electronic (q_e) and vibrational (q_v) components, which are as follows:

$$q_{tot} = q_t \times q_r \times q_e \times q_v$$
$$q_t = (2\pi Mk_B T / h^2)^{3/2} V; q_r = \pi^{1/2} / \sigma_r [T^{3/2} / (\Theta_{r,x} \Theta_{r,y} \Theta_{r,z})^{1/2}]; \quad (S13)$$
$$q_e = g_0; q_v = \prod_{i=1}^{3N-6} [1 / (1 - \exp^{-h\nu_i / k_B T})]$$

where M is the total mass; k_B is Boltzmann's constant; h is Planck's constant; V is volume; $\Theta_{r,x/y/z}$ are the characteristic rotational temperature in terms of moment of inertia; g_0 is the degeneracy of the energy level, which is essentially the spin multiplicity of the system under the approximation of *Gaussian* code; ν_i is the vibrational frequency associated with i^{th} mode.

Contributions to the internal thermal energy

The total energy (E_{tot}) is a summation of four components, namely, translational (E_t), rotational (E_r), electronic (E_e) and vibrational (E_v), which are as follows:

$$\begin{aligned}
E_{tot} &= E_t + E_r + E_e + E_v \\
E_t &= RT^2(\partial \ln q_t / \partial T)_V; E_r = RT^2(\partial \ln q_r / \partial T)_V; \\
E_e &= 0; E_v = R \sum_{i=1}^{3N-6} \exp^{h\nu_i/k_B T} [1/2 + 1/(\exp^{h\nu_i/k_B T} - 1)]
\end{aligned} \tag{S14}$$

Note that the thermal energy contribution of electronic component is zero because there is no temperature dependency in its respective partition function (see the expression of q_e in S13).

Contributions to the entropy

The total entropy (S_{tot}) is a summation of four components, namely, translational (S_t), rotational (S_r), electronic (S_e) and vibrational (S_v), which are as follows:

$$\begin{aligned}
S_{tot} &= S_t + S_r + S_e + S_v \\
S_t &= R(\ln q_t + 5/2); S_r = R(\ln q_r + T(\partial \ln q_r / \partial T)_V); \\
S_e &= R(\ln q_e + T(\partial \ln q_e / \partial T)_V); \\
S_v &= R \sum_{i=1}^{3N-6} [(\exp^{h\nu_i/k_B T} / (\exp^{h\nu_i/k_B T} - 1)) - \ln(1 - \exp^{h\nu_i/k_B T})]
\end{aligned} \tag{S15}$$

Note that the thermal energy contribution of electronic component is zero because there is no temperature dependency in its respective partition function (see the expression of q_e in S13).

- The ZPE-corrected electronic energy (E_{corr}) is the summation of electronic energy and zero-point energy (ZPE).
- The enthalpy (H) is the summation of (E_{corr}) and $k_B T$ (enthalpy correction) ; T is

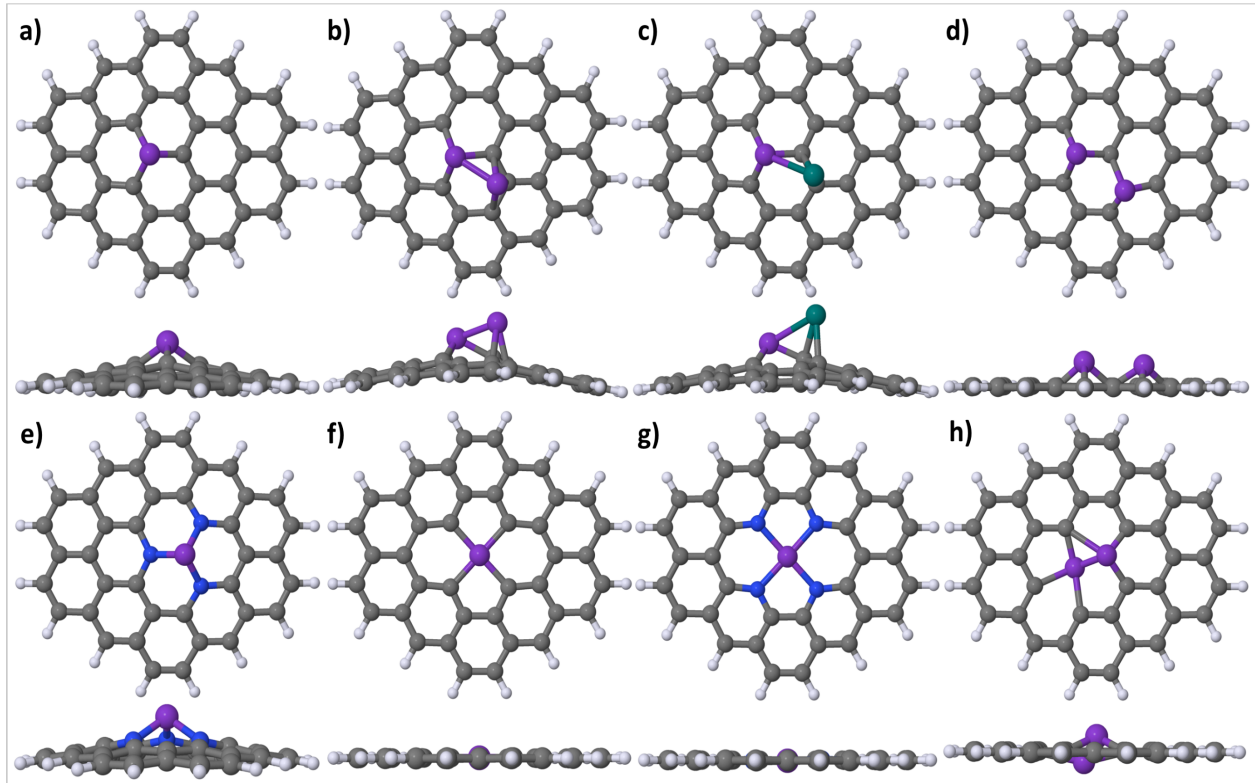


Figure S3: Various models of heteroatom doped graphene electrodes: a) M_SV, b) M₂_SV, c) MPt_SV, d) M₂_2SV, e) M_3N, f) M_DV, g) M_4N, and h) M₂_TV. The elements carbon, nitrogen and hydrogen are in grey, blue and lavender colors, respectively. The dopant atom is a model atom in purple color. The anchoring Pt atom in MPt_SV model is presented in teal color.

298.15 K.

- The Gibbs free energy is computed using $G = H - TS_{tot}$.

Theoretical equilibrium, limiting, and overpotential

The theoretical equilibrium potential is the potential at which initial and final states have equal free energies. The limiting potential is the applied electrode potential at which all energy steps are either exergonic or thermoneutral. The overpotential is a measure of the extra potential needed compared to the equilibrium potential and is calculated as the difference between equilibrium and limiting potentials.

Table S1: Mulliken charge on metal atom (q^M), magnetic moment (m) (eV) and stable spin multiplicity (SM) of heteroatom doped graphene models.

M	M_SV			M_3N			M_DV			M_4N		
	q^M	m	SM									
Ag	0.0	0.0	2	0.1	0.0	1	0.5	0.0	2	0.5	0.0	2
Al	1.3	0.0	2	0.5	0.0	1	1.8	0.0	2	1.9	0.0	2
Au	0.3	0.0	2	0.0	0.0	1	1.0	0.0	2	0.1	0.0	2
B	-0.6	0.0	2	1.1	0.1	3	0.1	0.0	2	2.5	0.0	2
Co	-0.8	0.0	2	0.1	0.5	3	0.3	0.0	2	0.4	0.0	2
Cu	-0.3	0.0	2	0.0	0.0	1	0.0	0.0	2	-0.1	0.0	2
Mn	0.0	0.5	4	0.4	1.0	7	0.3	0.8	6	0.3	0.4	4
N	0.1	0.0	2	0.5	0.0	1	0.6	0.0	2	-0.2	0.0	2
Rh	0.0	0.0	2	0.4	0.3	3	0.2	0.0	2	1.1	0.0	2
Cr	0.0	1.6	3	0.8	0.0	2	0.0	1.4	3	0.5	1.9	7
Fe	-0.7	0.0	1	0.4	0.5	4	-0.6	0.4	3	0.2	0.8	5
Mo	0.8	0.8	3	1.3	0.0	2	1.2	0.3	3	1.8	0.6	5
Ni	-0.7	0.0	1	0.0	0.0	2	-0.1	0.0	1	0.3	0.0	1
Pd	-0.5	0.0	1	0.1	0.0	2	-0.6	0.0	1	0.0	0.0	1
Pt	0.0	0.0	1	0.1	0.0	2	1.2	0.0	1	1.2	0.0	1
Ru	0.0	0.0	1	0.9	0.0	2	0.2	0.0	1	1.2	0.4	3
Zn	0.4	0.0	1	0.2	0.0	2	0.5	0.0	1	1.5	0.0	1

M	M ₂ -2SV				M ₂ -TV				M ₂ -SV				MPt ₂ -SV			
	q^{M_1}	q^{M_2}	m	SM	q^{M_1}	q^{M_2}	m	SM	q^{M_1}	q^{M_2}	m	SM	q^{M_1}	q^{Pt}	m	SM
Ag	-0.1	0.1	0.0	1	-0.2	0.3	0.0	1	0.0	0.0	0.0	1	0.0	0.7	0.0	2
Al	2.2	0.5	0.0	1	2.0	0.6	0.0	1	1.5	0.6	0.0	1	1.6	0.5	0.0	2
Au	-0.4	-0.8	0.0	1	0.2	-0.1	0.0	1	0.0	-0.3	0.0	1	-0.9	0.5	0.0	2
B	-0.4	-0.5	0.0	1	-0.2	-0.4	0.0	1	-0.4	0.2	0.0	1	-1.1	0.4	0.0	2
Co	-0.7	-0.7	0.1	3	-1.1	-0.9	0.6	3	-0.5	-0.1	1.0	3	-0.7	0.4	0.0	2
Cu	0.0	0.0	0.0	1	-0.9	-0.3	0.0	1	-0.1	-0.5	0.0	1	-0.5	0.7	0.0	2
Mn	-0.4	-0.4	1.6	5	-0.8	-0.6	1.9	7	-0.3	0.4	3.4	7	0.2	0.6	1.0	4
N	0.1	0.1	0.0	1	0.0	0.2	0.0	1	0.4	-0.5	0.0	1	0.4	0.5	0.0	2
Rh	0.0	0.0	0.2	3	0.0	0.0	0.0	1	0.0	0.1	0.0	1	0.1	0.5	0.0	2
Cr	-0.1	-0.1	0.8	3	-0.5	-0.5	0.1	3	0.0	0.3	2.4	3	0.2	0.6	1.0	3
Fe	-0.7	-0.7	0.4	3	-1.0	-0.9	1.8	5	-0.4	0.0	2.0	5	-0.1	0.7	0.6	3
Mo	0.6	0.6	0.0	1	1.2	0.7	0.0	1	0.6	0.5	1.7	3	1.1	0.3	0.5	3
Ni	-0.6	-0.6	0.0	1	-1.2	-0.6	0.0	1	-0.8	-0.2	0.0	1	-0.4	0.8	0.0	1
Pd	-0.5	-0.6	0.0	1	-0.3	-1.5	0.0	1	-0.4	0.0	0.0	1	-0.2	0.6	0.0	1
Pt	0.1	0.0	0.0	1	0.2	0.6	0.0	1	0.1	0.5	0.0	1	0.1	0.5	0.0	1
Ru	0.0	0.0	0.0	1	0.0	0.1	0.0	1	0.2	0.2	0.0	1	0.7	0.5	0.0	1
Zn	-0.3	0.0	0.0	1	-0.2	-0.1	0.0	1	0.3	0.1	0.0	1	0.5	0.2	0.0	1

Formation of M₂-SV and MPt-SV models

In the dimetallic (M₂-SV) models, heteroatom dimers occupies over a mono-vacant graphene site (see Figure S3). Similar to M₂-SV models, the bi-metallic MPt-SV electrodes (see Figure S3) are based on the anchoring of Pt atom on the metal site of M-SV models. In general, both the M₂-SV and MPt-SV electrodes are highly unstable and only three systems (B, Mn, and N dimers) are stable. Experimental evidence for the existence of MPt-SV and M₂-SV electrodes could not be found even though the results of a previous computational study⁷ suggest that the nucleation of homo- and heteroatoms over M-SV graphene sheets may take place. However, the absence of experimental evidence and computational results herein indicate that MPt-SV and M₂-SV are not likely to exist. Below, we do analyse the CO₂ binding over these models for academic interest and to compare them to other graphene systems.

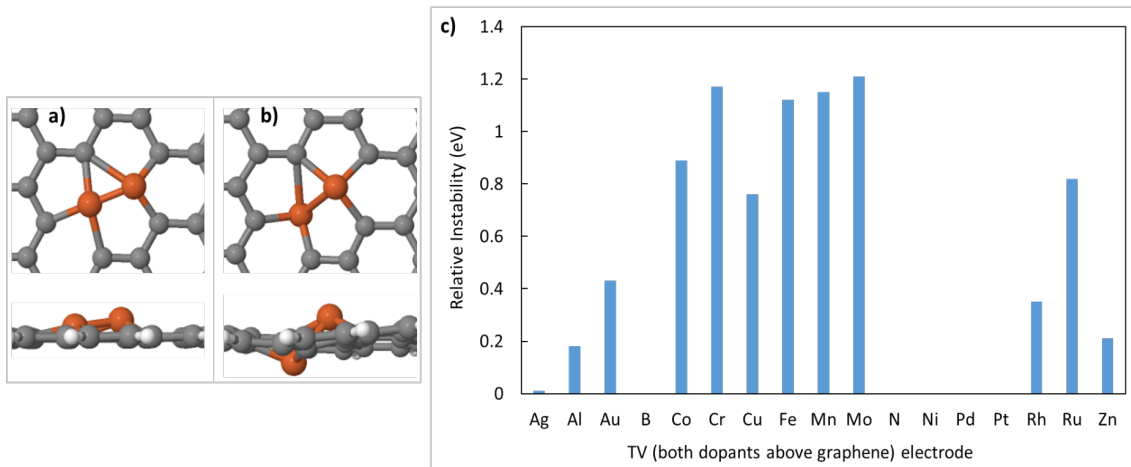


Figure S4: Sample optimized geometries of M₂-TV: (a) both dopants above the graphene plane (b) one atom above and one below the graphene plane, and (c) the relative instabilities of former.

Formation energetics

The formation energetics presented in Tables S2-S5 are based on eq. 1. The formation energy (Table S2) is computed by replacing G terms in eq. 1 as electronic energy (E). The formation energy corrected with ZPE (Table S3) is based on E_{corr} , i.e., free energies are replaced by E_{corr} . Table S4 presents formation enthalpy, which is computed using enthalpy ($H = E_{corr} + k_B T$) parameters. Finally, Table S5 presents free energies ($G = H - TS_{tot}$), which is computed using eq. 1.

Table S2: Formation energy (eV) of graphene based electrodes.

M	M_SV	M_3N	M_DV	M ₂ -2SV	M_4N	M ₂ -TV	M ₂ -SV	MPt_SV
Ag	0.48	-2.68	-2.54	-3.58	-2.72	0.01	1.41	0.27
Al	-1.66	-3.25	-5.50	-3.30	-3.70	-2.22	-0.20	0.33
Au	1.02	-2.32	-4.01	0.17	-2.65	-0.45	1.31	1.99
B	-7.63	-4.11	-6.45	-6.67	-3.49	-4.61	-1.68	-1.72
Co	-1.49	-2.60	-3.89	-1.66	-3.36	-1.18	0.56	0.73
Cu	0.08	-2.88	-4.05	-3.59	-3.29	-1.17	1.09	1.29
Mn	-3.09	-3.17	-5.62	-3.34	-3.79	-2.58	-0.99	-0.53
N	-7.26	-2.51	-4.65	-6.39	-2.66	-4.40	-1.51	-1.39
Rh	-1.63	-2.26	-3.70	-1.89	-3.17	-1.03	1.13	0.79
Cr	-0.63	-2.48	-3.11	-0.48	-3.19	0.47	1.21	1.05
Fe	-1.50	-2.87	-4.04	-1.97	-3.43	-1.71	0.31	0.29
Mo	0.41	-2.01	-2.70	-0.74	-2.65	0.26	2.99	1.40
Ni	-0.82	-2.78	-3.76	-1.38	-3.47	-1.57	0.82	0.55
Pd	-0.72	-2.53	-3.43	-1.19	-3.27	-1.58	0.46	0.73
Pt	-1.01	-2.19	-4.79	-1.59	-3.34	-1.97	0.54	0.54
Ru	-1.29	-2.24	-4.01	-1.74	-2.94	-0.55	2.08	1.14
Zn	-0.36	-3.12	-3.69	-2.75	-3.52	-1.24	-0.13	0.95

CO₂ bindings over M₂-SV, MPt-SV and M₂-TV models

On the M₂-SV and MPt-SV models, CO₂ is often activated during adsorption. The adsorption free energies are mostly exergonic or close to thermoneutral over both models except for Mn-, Fe-, and Mo-based MPt-SV (more than 2.5 eV). We excluded the M₂-SV and MPt-SV

Table S3: Formation energy (eV) corrected with zero-point energy (ZPE) of graphene based electrodes.

M	M_SV	M_3N	M_DV	M ₂ -2SV	M_4N	M ₂ -TV	M ₂ -SV	MPt_SV
Ag	0.88	-2.31	-1.94	-3.18	-2.33	0.36	1.61	0.48
Al	-1.25	-2.87	-4.92	-2.91	-3.30	-1.84	0.02	0.56
Au	1.40	-1.94	-3.38	0.50	-2.27	-0.06	1.53	2.19
B	-7.03	-3.69	-5.74	-6.12	-3.07	-4.10	-1.35	-1.41
Co	-1.07	-2.22	-3.28	-1.28	-2.96	-0.79	0.80	0.96
Cu	0.48	-2.51	-3.42	-3.17	-2.89	-0.81	1.29	1.50
Mn	-2.67	-2.78	-5.03	-2.95	-3.40	-2.19	-0.77	-0.30
N	-6.67	-2.10	-3.90	-5.82	-2.26	-3.85	-1.13	-1.06
Rh	-1.20	-1.89	-3.09	-1.52	-2.77	-0.66	1.36	1.01
Cr	-0.22	-2.11	-2.51	-0.09	-2.79	0.87	1.43	1.28
Fe	-1.06	-2.50	-3.42	-1.59	-3.03	-1.32	0.54	0.53
Mo	0.82	-1.65	-2.11	-0.36	-2.26	0.63	3.20	1.62
Ni	-0.40	-2.41	-3.13	-1.01	-3.06	-1.18	1.05	0.79
Pd	-0.30	-2.16	-2.85	-0.86	-2.87	-1.21	0.68	0.96
Pt	-0.60	-1.82	-4.19	-1.24	-2.94	-1.59	0.78	0.78
Ru	-0.85	-1.88	-3.37	-1.36	-2.54	-0.17	2.31	1.38
Zn	0.05	-2.74	-3.15	-2.39	-3.13	-0.91	0.09	1.17

Table S4: Formation enthalpy (eV) of graphene based electrodes.

M	M_SV	M_3N	M_DV	M ₂ -2SV	M_4N	M ₂ -TV	M ₂ -SV	MPt_SV
Ag	0.81	-2.35	-2.02	-3.19	-2.37	0.35	1.58	0.44
Al	-1.35	-2.92	-4.99	-2.94	-3.34	-1.87	-0.04	0.50
Au	1.34	-1.99	-3.47	0.48	-2.31	-0.09	1.49	2.15
B	-7.16	-3.75	-5.83	-6.19	-3.12	-4.16	-1.43	-1.48
Co	-1.17	-2.27	-3.36	-1.32	-3.00	-0.83	0.74	0.91
Cu	0.40	-2.55	-3.51	-3.19	-2.94	-0.83	1.25	1.46
Mn	-2.76	-2.84	-5.11	-2.98	-3.45	-2.22	-0.82	-0.35
N	-6.79	-2.16	-4.00	-5.89	-2.31	-3.91	-1.22	-1.14
Rh	-1.29	-1.94	-3.16	-1.55	-2.82	-0.69	1.30	0.96
Cr	-0.32	-2.16	-2.57	-0.13	-2.84	0.83	1.38	1.23
Fe	-1.16	-2.55	-3.49	-1.62	-3.07	-1.35	0.47	0.47
Mo	0.73	-1.70	-2.17	-0.39	-2.30	0.60	3.14	1.57
Ni	-0.49	-2.45	-3.22	-1.04	-3.11	-1.21	1.00	0.73
Pd	-0.39	-2.20	-2.92	-0.88	-2.92	-1.24	0.63	0.91
Pt	-0.68	-1.86	-4.27	-1.26	-2.98	-1.62	0.73	0.73
Ru	-0.95	-1.93	-3.45	-1.40	-2.59	-0.20	2.25	1.32
Zn	-0.03	-2.79	-3.21	-2.41	-3.17	-0.93	0.04	1.13

Table S5: Formation free energy (eV) of graphene based electrodes.

M	M_SV	M_3N	M_DV	M ₂ _2SV	M_4N	M ₂ _TV	M ₂ _SV	MPt_SV
Ag	1.41	-1.89	-1.43	-2.78	-1.94	0.79	2.05	0.95
Al	-0.66	-2.45	-4.42	-2.50	-2.89	-1.42	0.49	1.05
Au	1.94	-1.53	-2.83	0.98	-1.86	0.38	2.00	2.69
B	-6.47	-3.28	-5.28	-5.70	-2.68	-3.69	-0.87	-0.94
Co	-0.46	-1.79	-2.73	-0.81	-2.55	-0.33	1.30	1.47
Cu	1.02	-2.09	-2.88	-2.76	-2.49	-0.39	1.77	1.98
Mn	-2.08	-2.35	-4.47	-2.46	-2.99	-1.72	-0.29	0.20
N	-6.09	-1.68	-3.39	-5.37	-1.87	-3.45	-0.63	-0.55
Rh	-0.57	-1.47	-2.53	-1.03	-2.36	-0.18	1.88	1.53
Cr	0.39	-1.69	-1.96	0.40	-2.38	1.34	1.91	1.79
Fe	-0.42	-2.07	-2.85	-1.11	-2.62	-0.85	1.04	1.03
Mo	1.44	-1.22	-1.53	0.15	-1.84	1.13	3.72	2.13
Ni	0.20	-2.00	-2.58	-0.55	-2.65	-0.73	1.55	1.30
Pd	0.30	-1.75	-2.30	-0.42	-2.46	-0.77	1.16	1.46
Pt	0.04	-1.40	-3.59	-0.76	-2.52	-1.10	1.31	1.31
Ru	-0.19	-1.45	-2.79	-0.86	-2.12	0.31	2.85	1.90
Zn	0.60	-2.33	-2.70	-1.97	-2.74	-0.50	0.52	1.65

 Table S6: Magnetic moment (eV) and stable spin multiplicity (in the parenthesis) of CO₂ binding modified-graphene geometries.

M	M_SV	M_3N	M_DV	M ₂ _2SV	M_4N	M ₂ _TV	M ₂ _SV	MPt_SV
Ag	0.00 (2)	0.00 (1)	0.00 (2)	0.00 (1)	0.00 (2)	0.00 (1)	0.00 (1)	0.00 (2)
Al	0.00 (2)	0.00 (1)	0.00 (2)	0.00 (1)	0.00 (2)	0.00 (1)	0.00 (1)	0.00 (2)
Au	0.00 (2)	0.00 (1)	0.00 (2)	0.00 (1)	0.00 (2)	0.00 (1)	0.00 (1)	0.00 (2)
B	0.00 (2)	0.00 (1)	0.00 (2)	0.00 (1)	0.00 (2)	0.00 (1)	0.00 (1)	0.00 (2)
Co	0.00 (2)	0.00 (1)	0.00 (2)	0.00 (1)	0.00 (2)	0.00 (1)	0.09 (3)	0.00 (2)
Cu	0.00 (2)	0.00 (1)	0.00 (2)	0.00 (1)	0.00 (2)	0.00 (1)	0.00 (1)	0.00 (2)
Mn	0.00 (2)	0.04 (5)	0.41 (4)	0.86 (5)	0.13 (4)	2.83 (7)	2.06 (7)	0.16 (4)
N	0.00 (2)	0.00 (1)	0.00 (2)	0.00 (1)	0.00 (2)	0.00 (1)	0.00 (1)	0.00 (2)
Rh	0.00 (2)	0.00 (1)	0.00 (2)	0.00 (1)	0.00 (2)	0.00 (1)	0.00 (1)	0.00 (2)
Cr	0.38 (3)	0.02 (4)	0.35 (3)	1.11 (3)	0.72 (3)	1.38 (3)	2.01 (3)	1.28 (3)
Fe	0.00 (1)	0.41 (4)	1.83 (5)	0.00 (1)	0.00 (1)	1.68 (5)	1.08 (3)	0.34 (3)
Mo	0.00 (1)	0.00 (2)	0.00 (1)	0.00 (1)	0.00 (1)	0.00 (1)	0.00 (1)	0.58 (3)
Ni	0.00 (1)	0.00 (2)	0.00 (1)	0.00 (1)	0.00 (1)	0.00 (1)	0.00 (1)	0.00 (1)
Pd	0.00 (1)	0.00 (2)	0.00 (1)	0.00 (1)	0.00 (1)	0.00 (1)	0.00 (1)	0.00 (1)
Pt	0.00 (1)	0.00 (2)	0.00 (1)	0.00 (1)	0.00 (1)	0.00 (1)	0.00 (1)	0.00 (1)
Ru	0.00 (1)	0.00 (2)	0.00 (1)	0.00 (1)	0.00 (1)	0.00 (1)	0.00 (1)	0.00 (1)
Zn	0.00 (1)	0.00 (2)	0.00 (1)	0.00 (1)	0.00 (1)	0.00 (1)	0.00 (1)	0.00 (1)

electrodes from further studies as their formations are thermodynamically unstable and they have not been experimentally observed.

Among the $M_2\text{-TV}$ electrodes, only Zn, Cu, and Al derivatives spontaneously bind and activate CO_2 . The charge transfer by $\text{Al}_2\text{-TV}$ electrode to the CO_2 molecule is reported as $\sim -0.3\text{e}$, whereas, over Cu and Zn electrodes, rather high charge transfer ($\sim -0.8\text{ e}$) is observed. Other $M_2\text{-TV}$ electrodes are either unable to bind or activate CO_2 .

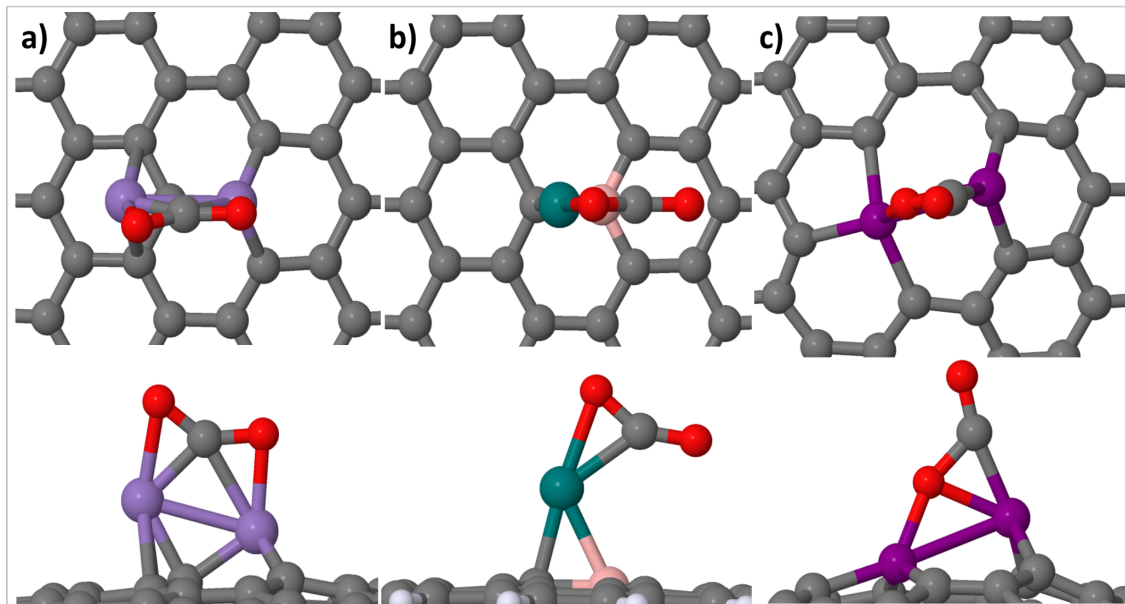


Figure S5: The optimized binding geometries of CO_2 over: a) $\text{Mn}_2\text{-SV}$, b) $\text{BPt}\text{-SV}$, and c) $\text{Al}_2\text{-TV}$. The elements carbon, oxygen, and nitrogen are in grey, red, and blue colors, respectively.

Adsorption energetics

The adsorption energetics presented in Tables S7-S10 are based on eq. 2. The adsorption energy (Table S7) is computed using the electronic energy instead of free energy, as presented in eq. 2. The adsorption energy corrected with ZPE (Table S8) is computed by replacing G in eq. 2 as E_{corr} . Table S9 presents adsorption enthalpy, which is computed using enthalpy ($H = E_{corr} + k_B T$) parameters. Finally, Table S10 presents free energies, which is computed according to eq. 2.

Table S7: Adsorption energy (eV) of CO₂ over heteroatom modified graphene based electrodes.

M	M_SV	M_3N	M_DV	M ₂ -2SV	M_4N	M ₂ -TV	M ₂ -SV	MPt_SV
Ag	-0.34	-0.26	-0.20	-0.36	-0.19	-0.39	-0.36	-0.29
Al	-0.31	-0.73	-0.28	-0.85	0.18	-1.06	-0.30	-0.90
Au	0.56	-0.25	-0.21	-6.94	-0.19	0.00	-0.32	-0.54
B	-0.22	0.47	-0.44	-1.04	0.50	-0.24	-1.06	-0.70
Co	-0.32	-1.08	-0.19	-0.74	-0.24	0.64	-0.64	-1.00
Cu	0.18	-0.31	-0.18	-0.55	-0.17	-0.92	-0.57	-1.10
Mn	-0.13	-0.25	-0.23	-0.77	0.50	-0.15	-1.27	3.43
N	-0.20	-0.47	-0.23	-0.85	-0.37	0.51	-0.33	-0.63
Rh	-0.28	-1.12	-0.20	-0.36	-0.23	0.63	-1.19	-0.63
Cr	-0.67	-0.93	0.97	-1.94	0.02	-0.25	-1.54	-1.49
Fe	-0.50	-0.95	-0.50	-0.54	0.35	1.33	-0.73	2.08
Mo	-0.22	-1.23	-0.14	-1.18	-1.42	-0.32	-1.30	2.67
Ni	-0.33	-0.89	-0.18	-3.15	-0.18	-0.48	-1.06	-0.55
Pd	-0.30	-0.39	-0.19	-0.32	-0.21	-0.42	-0.41	-0.57
Pt	-0.27	-1.26	-0.21	-0.22	-0.26	-0.46	-0.50	-0.50
Ru	-0.36	-0.85	-0.26	-0.53	-0.41	0.35	-1.63	-1.18
Zn	-0.47	-0.07	-0.23	-3.14	-0.22	-1.99	-0.33	-1.03

Table S8: Adsorption energy (eV) corrected with zero-point energy (ZPE) of CO₂ over heteroatom modified graphene based electrodes.

M	M_SV	M_3N	M_DV	M ₂ -2SV	M_4N	M ₂ -TV	M ₂ -SV	MPt_SV
Ag	-0.32	-0.24	-0.18	-0.32	-0.18	-0.38	-0.33	-0.25
Al	-0.28	-0.68	-0.24	-0.80	0.22	-1.04	-0.27	-0.89
Au	0.55	-0.21	-0.18	-6.75	-0.16	0.01	-0.29	-0.52
B	-0.20	0.56	-0.44	-1.02	0.52	-0.23	-1.00	-0.69
Co	-0.28	-1.00	-0.17	-0.66	-0.23	0.72	-0.58	-0.94
Cu	0.17	-0.29	-0.17	-0.56	-0.15	-0.81	-0.53	-1.06
Mn	-0.11	-0.18	-0.21	-0.70	0.55	-0.04	-1.25	3.43
N	-0.17	-0.37	-0.22	-0.82	-0.34	0.53	-0.30	-0.63
Rh	-0.26	-1.04	-0.18	-0.31	-0.22	0.69	-1.15	-0.60
Cr	-0.64	-0.87	1.01	-1.90	0.11	-0.25	-1.49	-1.44
Fe	-0.51	-0.84	-0.49	-0.46	0.43	1.34	-0.66	2.12
Mo	-0.17	-1.17	-0.09	-1.16	-1.34	-0.29	-1.22	2.71
Ni	-0.29	-0.82	-0.17	-3.04	-0.16	-0.44	-1.02	-0.53
Pd	-0.30	-0.35	-0.17	-0.29	-0.16	-0.39	-0.38	-0.56
Pt	-0.24	-1.20	-0.17	-0.17	-0.24	-0.43	-0.48	-0.48
Ru	-0.33	-0.73	-0.23	-0.46	-0.34	0.39	-1.55	-1.12
Zn	-0.44	-0.08	-0.20	-3.02	-0.20	-1.90	-0.31	-1.00

Table S9: Adsorption enthalpy (eV) of CO₂ over heteroatom modified graphene based electrodes.

M	M_SV	M_3N	M_DV	M ₂ -2SV	M_4N	M ₂ -TV	M ₂ -SV	MPt_SV
Ag	-0.30	-0.22	-0.16	-0.32	-0.15	-0.36	-0.31	-0.24
Al	-0.27	-0.69	-0.23	-0.83	0.23	-1.06	-0.26	-0.89
Au	0.58	-0.22	-0.16	-6.73	-0.14	0.04	-0.27	-0.52
B	-0.18	0.54	-0.45	-1.00	0.52	-0.20	-1.00	-0.69
Co	-0.27	-1.01	-0.15	-0.69	-0.21	0.69	-0.60	-0.96
Cu	0.19	-0.27	-0.14	-0.56	-0.15	-0.85	-0.51	-1.07
Mn	-0.11	-0.19	-0.18	-0.73	0.56	-0.06	-1.26	3.43
N	-0.15	-0.39	-0.19	-0.80	-0.32	0.55	-0.28	-0.61
Rh	-0.24	-1.06	-0.16	-0.33	-0.20	0.67	-1.16	-0.63
Cr	-0.65	-0.87	1.00	-1.92	0.09	-0.26	-1.51	-1.45
Fe	-0.50	-0.86	-0.49	-0.48	0.41	1.32	-0.67	2.10
Mo	-0.18	-1.17	-0.10	-1.17	-1.35	-0.29	-1.24	2.70
Ni	-0.28	-0.84	-0.17	-3.05	-0.14	-0.43	-1.03	-0.53
Pd	-0.27	-0.35	-0.15	-0.28	-0.13	-0.38	-0.39	-0.56
Pt	-0.22	-1.22	-0.16	-0.18	-0.22	-0.42	-0.48	-0.48
Ru	-0.32	-0.73	-0.21	-0.48	-0.35	0.37	-1.57	-1.14
Zn	-0.43	-0.06	-0.18	-3.04	-0.18	-1.92	-0.29	-1.01

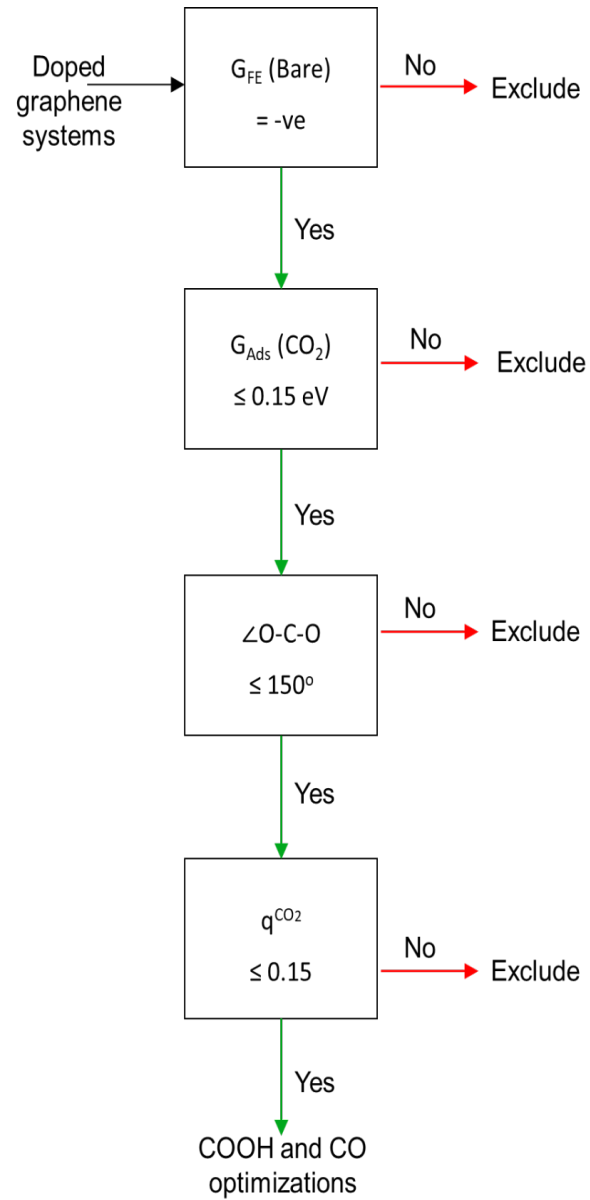


Figure S6: The flow-chart of a four-level selection criteria to study the electrocatalytic CO₂RR.

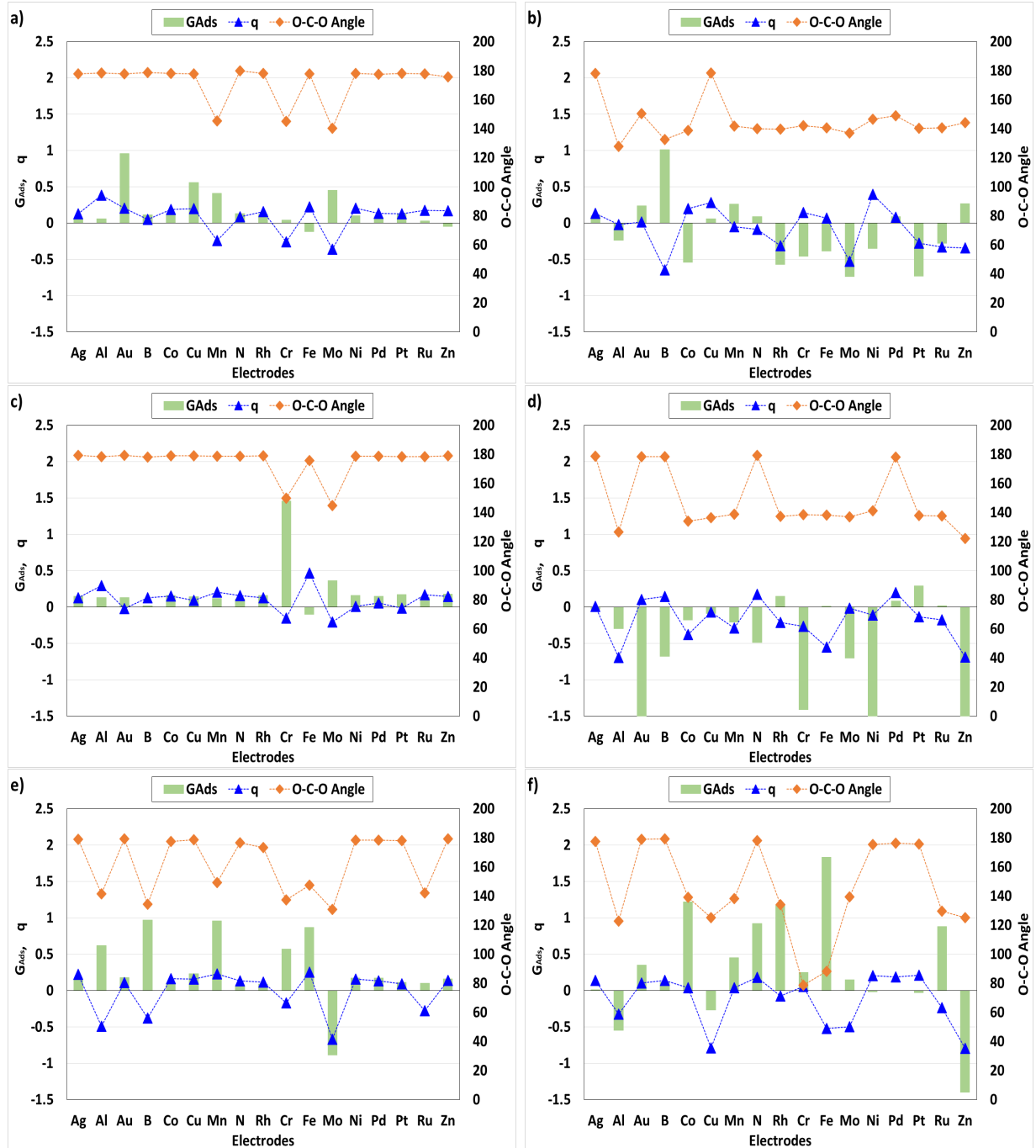


Figure S7: The parametric details, namely, adsorption free energies of CO₂ (G_{Ads}), net charge transfer (q), and O–C–O angle, for the selection criteria over the considered electrodes: a) M_{SV}, b) M_{3N}, c) M_{DV}, d) M_{2SV}, e) M_{24N}, and f) M_{2TV}. The M_{2-SV} and MPt_{SV} electrodes are omitted from electrocatalytic CO₂RR thermodynamics because of their high instabilities.

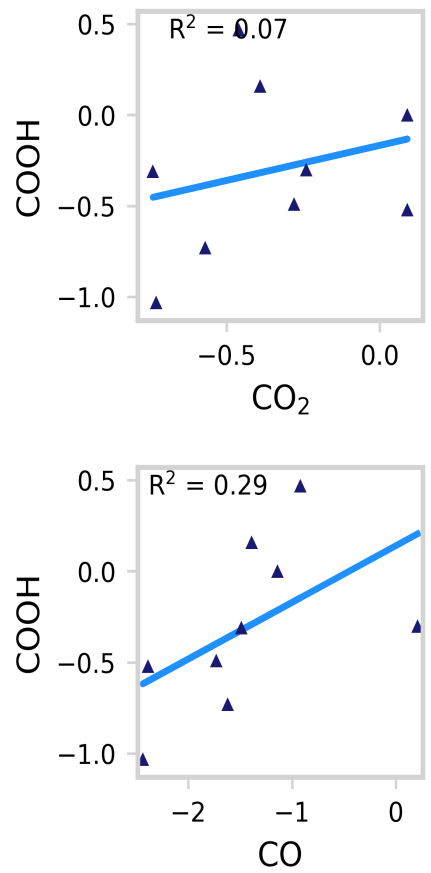


Figure S8: Linear scaling relationships between the binding free energies of COOH *vs.* CO₂ and COOH *vs.* CO over M₃N electrodes.

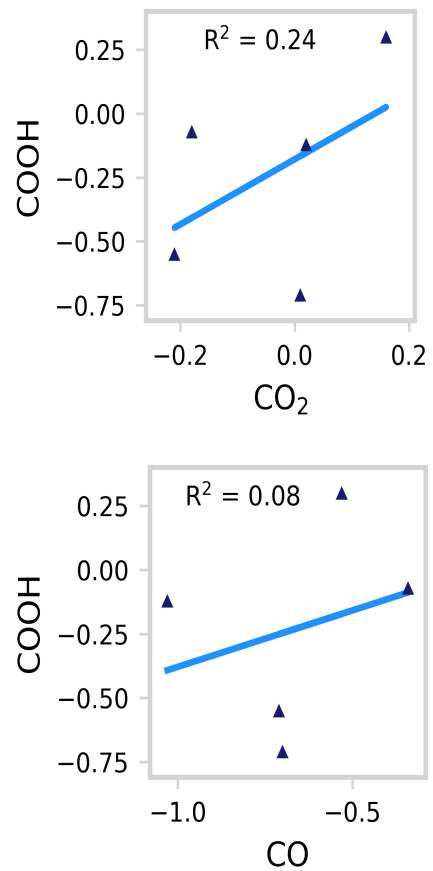


Figure S9: Linear scaling relationships between the binding free energies of COOH *vs.* CO₂ and COOH *vs.* CO over M₂-2SV electrodes.

Table S10: Adsorption free energy (eV) of CO₂ over heteroatom modified graphene based electrodes.

M	M_SV	M_3N	M_DV	M ₂ -2SV	M_4N	M ₂ -TV	M ₂ -SV	MPt_SV
Ag	0.06	0.10	0.15	-0.03	0.14	0.01	0.04	0.13
Al	0.06	-0.24	0.13	-0.30	0.62	-0.55	0.07	-0.45
Au	0.96	0.24	0.13	-6.50	0.18	0.35	0.09	-0.12
B	0.11	1.01	0.02	-0.68	0.97	0.11	-0.59	-0.30
Co	0.11	-0.54	0.16	-0.18	0.10	1.22	-0.09	-0.51
Cu	0.56	0.06	0.14	-0.09	0.23	-0.27	-0.17	-0.65
Mn	0.33	0.26	0.12	-0.21	0.96	0.45	-0.77	3.89
N	0.13	0.09	0.11	-0.49	0.06	0.92	0.06	-0.25
Rh	0.12	-0.57	0.16	0.15	0.09	1.17	-0.72	-0.14
Cr	-0.20	-0.46	1.46	-1.41	0.57	0.25	-0.99	-0.98
Fe	-0.12	-0.39	-0.10	0.01	0.87	1.83	-0.13	2.59
Mo	0.31	-0.74	0.36	-0.70	-0.89	0.15	-0.68	3.18
Ni	0.10	-0.35	0.16	-2.62	0.17	-0.02	-0.59	-0.12
Pd	0.07	0.09	0.15	0.08	0.17	0.00	0.07	-0.14
Pt	0.13	-0.73	0.17	0.29	0.11	-0.03	-0.07	-0.07
Ru	0.03	-0.28	0.13	0.02	0.10	0.88	-1.07	-0.67
Zn	-0.05	0.27	0.18	-2.63	0.16	-1.40	0.07	-0.54

Table S11: The binding free energies (eV) of COOH and CO over considered electrodes.

Electrode	M											
	Al	Co	Cu	Mn	N	Rh	Cr	Fe	Mo	Pd	Pt	Ru
M_3N	COOH	-0.30	--	--	-0.52	-0.73	0.47	0.16	-0.31	0.00	-1.03	-0.49
	CO	0.21	--	--	-2.39	-1.62	-0.92	-1.39	-1.49	-1.14	-2.44	-1.73
M₂-2SV	COOH	--	-0.07	--	-0.55	--	0.30	--	-0.71	--	--	-0.12
	CO	--	-0.34	--	-0.71	--	-0.53	--	-0.70	--	--	-1.03
M_4N	COOH	--	--	--	--	--	--	--	-0.43	--	--	-0.36
	CO	--	--	--	--	--	--	--	-1.31	--	--	-1.83
M₂-TV	COOH	-0.27	--	0.97	--	--	--	--	--	--	--	0.52
	CO	-0.10	--	0.12	--	--	--	--	--	--	--	-0.86

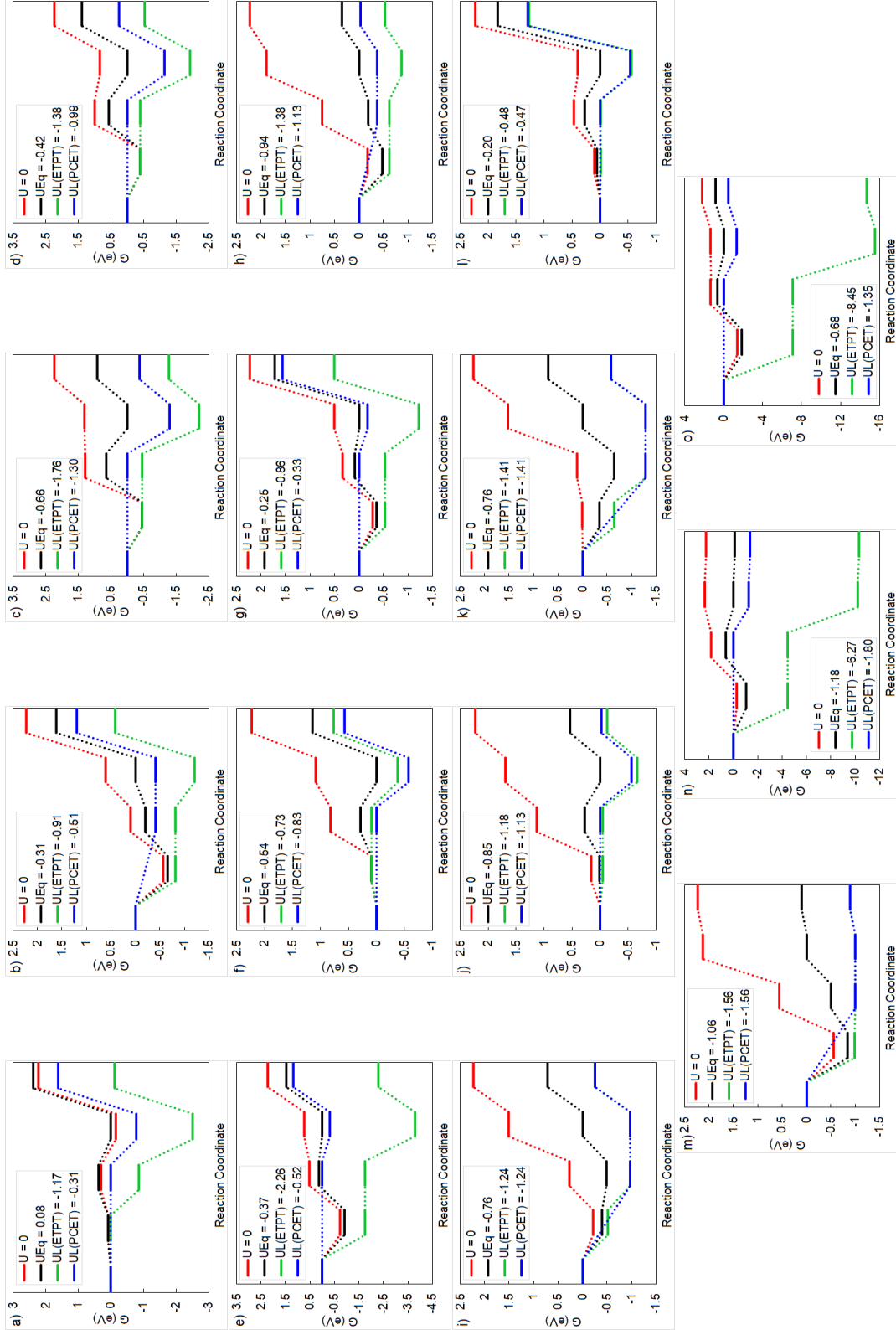


Figure S10: Electrochemical thermodynamics of CO_2 reduction reaction using PCET and ETPT mechanisms over graphene electrodes: a) N_3N, b) Rh_3N, c) Cr_3N, d) Fe_3N, e) Mo_3N, f) Pd_3N, g) Ru_3N, h) Co_2_2SV, i) Mn_2_2SV, j) Rh_2_2SV, k) Fe_2_2SV, l) Ru_4N, m) Al_2_TV, n) Cu_2_TV, and o) Zn_2_TV. The representation of x-axis is similar to as described in main manuscript.

Table S12: Calculated potentials (V) of electrocatalytic CO₂ reduction reaction to produce CO over selected electrodes using PCET and ETPT mechanisms.

Electrode	Potential (V)	M											
		Al	Co	Cu	Mn	N	Rh	Cr	Fe	Mo	Pd	Pt	Ru
M_3N	U_{Eq}	-1.22	—	—	—	0.08	-0.31	-0.66	-0.42	-0.37	-0.54	0.11	-0.25
	U_L (ETPT)	-1.91	—	—	—	-1.17	-0.91	-1.76	-1.38	-2.26	-0.73	-0.69	-0.86
	U_L (PCET)	-1.91	—	—	—	-0.31	-0.51	-1.30	-0.99	-0.52	-0.83	0.00	-0.33
	U_{Op} (ETPT)	0.69	—	—	—	1.25	0.61	1.10	0.96	1.89	0.19	0.80	0.61
	U_{Op} (PCET)	0.69	—	—	—	0.39	0.21	0.65	0.57	0.15	0.29	0.11	0.08
	U_{Eq}	—	-0.94	—	-0.76	—	-0.85	—	-0.76	—	—	-0.60	—
M₂_2SV	U_L (ETPT)	—	-1.38	—	-1.24	—	-1.18	—	-1.41	—	—	—	-0.81
	U_L (PCET)	—	-1.13	—	-1.24	—	-1.13	—	-1.41	—	—	—	-0.71
	U_{Op} (ETPT)	—	0.43	—	0.48	—	0.33	—	0.64	—	—	—	0.21
	U_{Op} (PCET)	—	0.19	—	0.48	—	0.28	—	0.64	—	—	—	0.10
	U_{Eq}	—	—	—	—	—	—	—	—	-0.46	—	—	-0.20
	U_L (ETPT)	—	—	—	—	—	—	—	-2.96	—	—	—	-0.48
M_4N	U_L (PCET)	—	—	—	—	—	—	—	-0.52	—	—	—	-0.47
	U_{Op} (ETPT)	—	—	—	—	—	—	—	2.50	—	—	—	0.28
	U_{Op} (PCET)	—	—	—	—	—	—	—	0.06	—	—	—	0.27
	U_{Eq}	-1.06	—	-1.18	—	—	—	—	—	—	—	—	-0.68
	U_L (ETPT)	-1.56	—	-6.27	—	—	—	—	—	—	—	—	-8.45
	U_L (PCET)	-1.56	—	-1.80	—	—	—	—	—	—	—	—	-1.35
M₂_TV	U_{Op} (ETPT)	0.50	—	5.10	—	—	—	—	—	—	—	—	7.76
	U_{Op} (PCET)	0.50	—	0.63	—	—	—	—	—	—	—	—	0.66

References

- (1) Bratsch, S. G. Standard Electrode Potentials and Temperature Coefficients in Water at 298.15 K. *J. Phys. Chem. Ref. Data* **1989**, *18*, 1–21.
- (2) Melander, M. M.; Kuisma, M. J.; Christensen, T. E. K.; Honkala, K. Grand-canonical approach to density functional theory of electrocatalytic systems: Thermodynamics of solid-liquid interfaces at constant ion and electrode potentials. *J. Chem. Phys.* **2019**, *150*, 041706.
- (3) Trasatti, S. The “absolute” electrode potential—the end of the story. *Electrochim. Acta* **1990**, *35*, 269 – 271.
- (4) Nørskov, J. K.; Rossmeisl, J.; Logadottir, A.; Lindqvist, L.; Kitchin, J. R.; Bligaard, T.; Jónsson, H. Origin of the Overpotential for Oxygen Reduction at a Fuel-Cell Cathode. *J. Phys. Chem. B* **2004**, *108*, 17886–17892.
- (5) Schmickler, W.; Guidelli, R. The partial charge transfer. *Electrochim. Acta* **2014**, *127*, 489 – 505.
- (6) Vijay, S.; Gauthier, J. A.; Heenen, H. H.; Bukas, V. J.; Kristoffersen, H. H.; Chan, K. Dipole-Field Interactions Determine the CO₂ Reduction Activity of 2D Fe-N-C Single-Atom Catalysts. *ACS Catal.* **2020**, *10*, 7826–7835.
- (7) Ferrante, F.; Prestianni, A.; Cortese, R.; Schimmenti, R.; Duca, D. Density functional theory investigation on the nucleation of homo-and heteronuclear metal clusters on defective graphene. *J. Phys. Chem. C* **2016**, *120*, 12022–12031.